We are IntechOpen,
the world's leading publisher of
Open Access books
Built by scientists, for scientists

6,900
Open access books available

185,000
International authors and editors

200M
Downloads

Our authors are among the

154
Countries delivered to

TOP 1%
most cited scientists

12.2%
Contributors from top 500 universities

CLARIVATE ANALYTICS
BOOK CITATION INDEX
INDEXED

WEB OF SCIENCE™

Selection of our books indexed in the Book Citation Index
in Web of Science™ Core Collection (BKCI)

Interested in publishing with us?
Contact book.department@intechopen.com

Numbers displayed above are based on latest data collected.
For more information visit www.intechopen.com

Slot-Line UWB Bandpass Filters and Band-Notched UWB Filters

Xuehui Guan

Additional information is available at the end of the chapter

Abstract

Slot-line ultra-wideband (UWB) bandpass filters and band-notched UWB filters are presented for UWB systems. Three types of slot-line multimode resonators are proposed and studied. Microstrip feed lines are used to realize the desired strong external coupling in a simple manner. By properly allocating the resonant modes of resonator and external coupling, UWB bandpass filters have been realized. Next, microstrip resonators, i.e., open-loop resonator, stub-loaded dual-mode resonator, and triangular dual-mode ring resonator, are loaded to the slot-line; notched bands are realized in the UWB passbands. The design methodology has been verified by the measured results.

Keywords: stepped-impedance resonator, notch band, stub-loaded resonator, slot-line resonator, multimode resonator

1. Introduction

Ultra-wideband (UWB) technology is strongly desired in high-speed transmission systems. Since the US Federal Communications Commission (FCC) authorized the unlicensed use of UWB devices in 2002 [1], research on UWB components such as UWB bandpass filters (BPFs) becomes a hot spot. Many methods have been proposed to design various UWB bandpass filters (BPFs) including multimode resonators (MMRs) [2] and stub-loaded resonators [3, 4]. To achieve the desired external coupling, extreme narrow gap between microstrip resonator and I/O feed lines is necessarily needed, which increases the difficulty of manufacturing. To keep the gap width in a moderate scale that can be realized easily by using PCB process, an aperture-backed parallel-coupled microstrip line with enhanced coupling degree is constructed to allocate the coupling peak [5, 6]. For the indoor and handheld UWB systems, the

FCC required that the UWB bandwidth must be strictly contained between 3.1 and 10.6 GHz. However, there is a need to avoid the interference from existing wireless communication systems such as wireless local area network (WLAN) in 5.2-GHz band. Generating a notch band in a UWB BPF is an effective and feasible method to solve this problem. As usual, an external resonator is used to create a notch band in the core of the UWB BPF at the cost of enlarged size [7]. In [8, 9], a stepped-impedance resonator (SIR) is embedded to achieve a band-notched characteristic without increasing the circuit size. Band-notched filtering effect was achieved by adding a meander line slot to reject the undesired WLAN radio signals [10]. In [11], two spurline sections are employed to create a sharp band-notched filter for suppressing the signals of 5-GHz WLAN devices. In [12], a dual-mode fractal defected-ground structure (DGS) bandstop filter is realized and connected with MMR; band-notched characteristics are realized. To avoid the interference of the wireless local area network (WLAN) at 5.25 and 5.775 GHz, two different quarter-wavelength lines are arranged on the ground of UWB BPF to generate dual narrow stopbands [13]. Obviously, combined bottom layer and top layer can make fully use of the circuit board, increasing the coupling between resonator and feed line, while keeping the circuit size [14].

In this chapter, slot-line multimode resonators are studied and applied in UWB BPFs. Microstrip feed lines are used to realize the desired external coupling in a simple manner. Microstrip resonators, such as open-loop resonator, stub-loaded dual-mode resonator, and square ring dual-mode resonator, are loaded to the slot-line; notch bands are realized in the UWB passbands.

2. Open-loop resonator-loaded slot UWB filter

2.1. Stepped-impedance slot-line UWB BPF

A diagram of the original UWB BPF using stepped-impedance slot-line resonator is shown in **Figure 1**. A multimode resonator is realized by using the stepped-impedance slot-line on the ground plane. By setting the impedance ratio and the length of the slot-line resonator, the first three resonant modes are equally allocated in the UWB passband. In other words, the
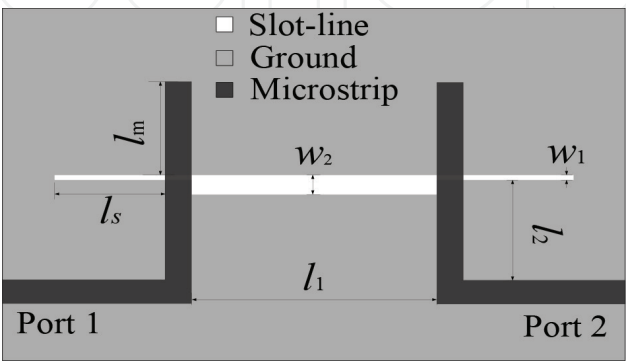

Figure 1. The schematic of original UWB filter using stepped-impedance slot-line resonator.

central resonant frequency of the multimode slot-line resonator is determined by the length l_1; the location of first and third resonant frequency is determined by the width ratio w_2/w_1. l_s is approximately $\lambda_g/4$ of slot-line in center frequency, and l_m is approximately $\lambda_g/4$ of microstrip line in center frequency. To decrease the return loss in the passband of UWB, the coupling must be very strong, and microstrip feed lines are placed right on the top and orthogonal to the slot-line resonator.

2.2. Band-notched UWB filter

To effectively decrease the interference between UWB system and WLAN system, a notch band shall be produced in the UWB band. To avoid the size increment of the circuit, the open-loop resonator is placed right on the top of stepped-impedance slot-line resonator, and the circuit volume can be fully used. **Figure 2(a)** shows the physical layout of an open-loop resonator-loaded slot-line. Frequently used structures for creating notch band include conventional open stub, spurline, embedded open stub (EOS), and open-loop resonator (OLR). **Figure 3** provides a comparison of transmission characteristic at 5.25 GHz between these methods. Open-loop resonator can produce the sharpest notch band, and conventional open stubs produce the widest notch band. The spurline and embedded stub do not increase the size of the circuit, while open-loop resonator and conventional open stub may increase the circuit size. With respect to that, the WLAN passband is quite narrow, the transition band shall be very sharp, and the open-loop resonator is preferred.

The microstrip open-loop resonator provides a bypass for the signal at its resonant frequency, and a notch band is produced. The resonant frequency of the open-loop resonator is approximated by

$$f_1 = \frac{c}{2\sqrt{\varepsilon_{eff}}(4a - g)} \tag{1}$$

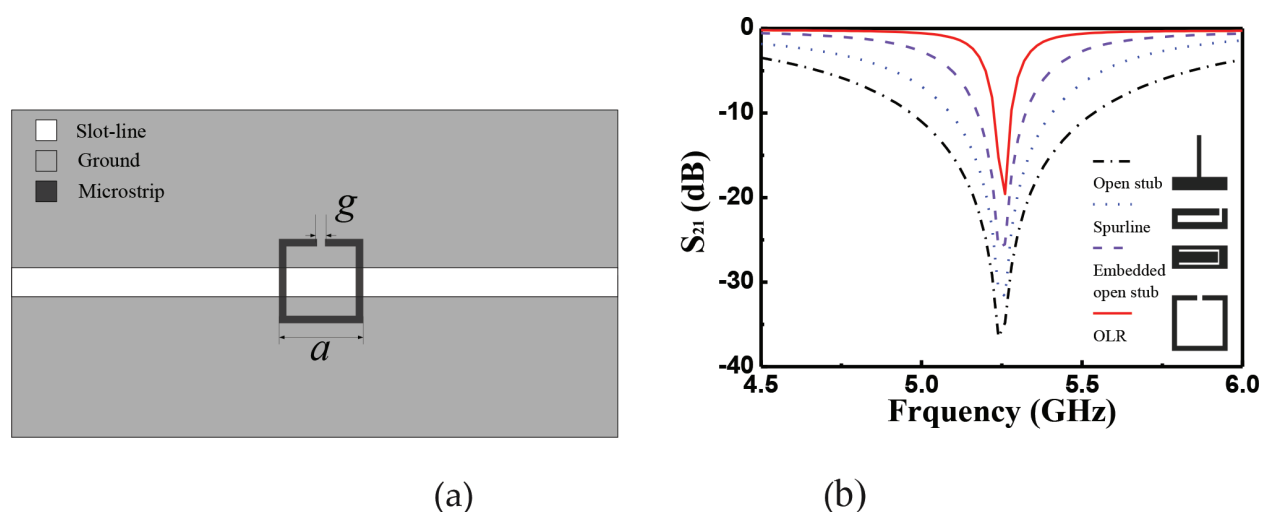(a)   (b)

Figure 2. (a) Open-loop resonator-loaded slot-line resonator and (b) simulated frequency responses of the four frequently used structures.

where c is the speed of light in vacuum, ε_{eff} is the effective dielectric constant, and a and g are the side length and the gap width of the microstrip open-loop resonator, respectively.

2.3. Experimental results and discussions

A UWB BPF with notch band is designed based on the abovementioned method. To further increase the attenuation of the notch band in the UWB band, two microstrip open-loop resonators are loaded to the slot-line resonator. By proper setting the position of the two open-loop resonators, a narrow notch band can be achieved in the UWB passband. The layout of the proposed notched UWB BPF is shown in **Figure 3(a)**. **Figure 3(b)** illustrates a full-wave

(a)   (b)
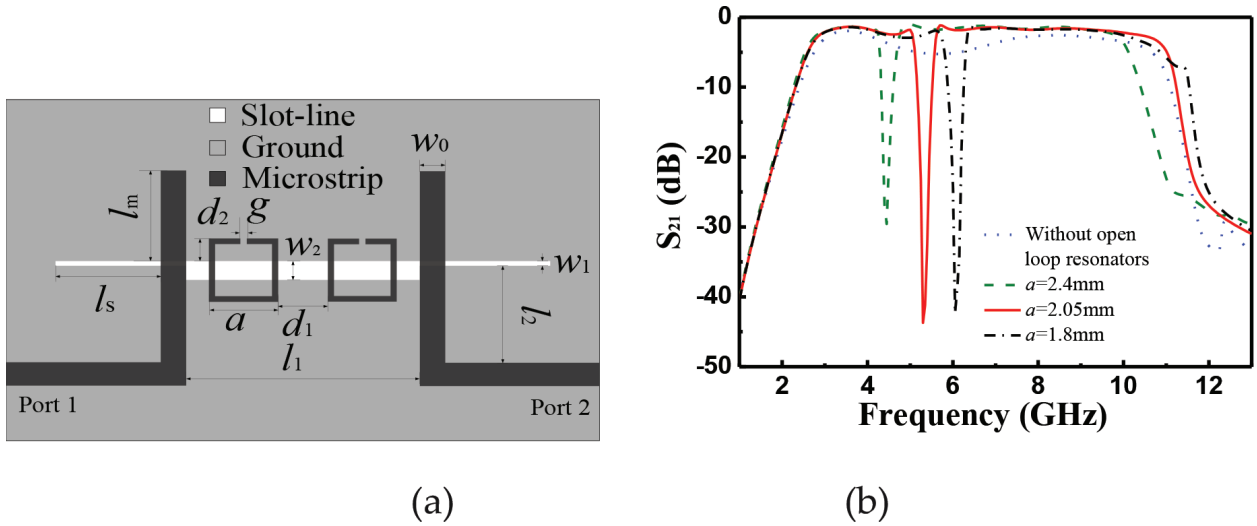
Figure 3. (a) Layout of the proposed band-notched UWB BPF using open-loop resonator-loaded stepped-impedance slot-line resonator and (b) simulated result of the band-notched UWB BPF with varying a.
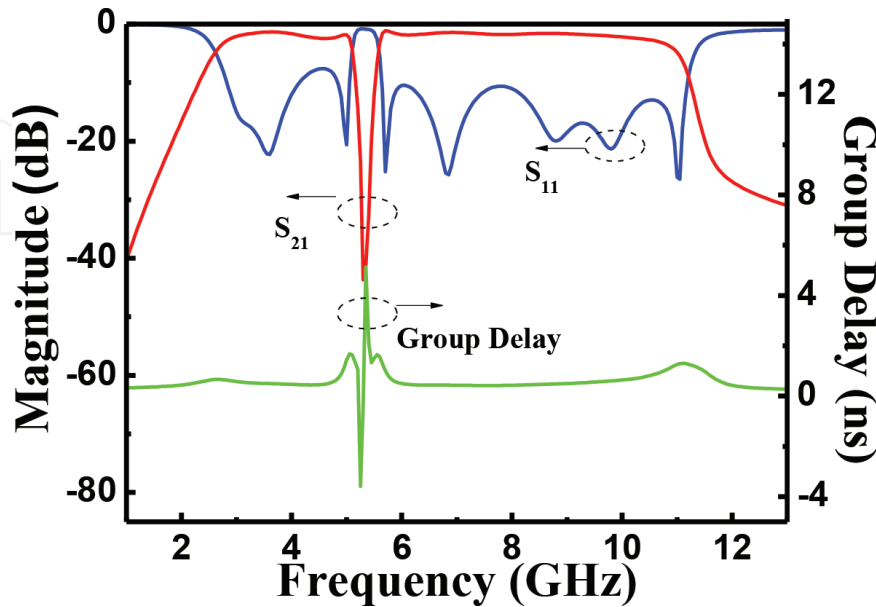

Figure 4. Measured frequency responses of proposed band-notched UWB BPF using open-loop resonator-loaded stepped-impedance slot-line resonator.

simulated result of the location of notch band against the side length a. Increment of slot-line width will increase the insertion loss in the passband. It is also observed that loaded microstrip open-loop resonator produces a notch band and decreases the insertion loss in the passband.

The UWB bandpass filter with improved performance is designed, fabricated, and measured. A substrate with relative dielectric constant of $\varepsilon_r = 4.5$ and a thickness of h = 0.8 mm is used in the design. The parameters of the proposed filter in **Figure 3** are $l_1 = 12$ mm, $l_2 = 5.6$ mm, $l_s = 6.2$ mm, $l_m = 5.9$ mm, $w_0 = 1.5$ mm, $w_3 = 0.2$ mm, $w_4 = 1.2$ mm, $w_r = 0.2$ mm, $d_1 = 1.9$ mm, $d_2 = 1.55$ mm, $a = 4.1$ mm, and $g = 0.2$ mm. Measured frequency responses of the filter are plotted in **Figure 4**. The results exhibit attractive UWB bandpass behaviors in the 3.1–10.6-GHz band; the narrow notch band locates in 5-GHz band. Its insertion is greater than 29 dB and the 3-dB bandwidth is about 300 MHz. The insertion loss is about 1.2 dB at the center frequency of 6.85 GHz. The group delay is below 2 ns within the passband.

3. UWB BPF with three-stub-loaded slot-line multiple mode resonator (MMR)

3.1. Three-stub-loaded slot-line UWB BPF

Figure 5 shows the configurations of the proposed UWB BPF with three-stub-loaded slot-line MMR. Three-stub-loaded slot-line MMR is fed by microstrip feed line. The MMR and the feed lines are folded and orthogonal coupling is applied.

The slot-line MMR consists of a stepped-impedance resonator and three loading stubs, with one located at the middle of the resonator. Compared with traditional SIR and stub-loaded resonator (SLR), the proposed one has more degrees of freedom to control its resonant frequencies. Once the original parameters of the slot-line resonator are determined, EM solver is invoked to tune the structure to achieve an optimized characteristic. **Figure 6** depicts the simulated transmission characteristics of the resonator with and without additional stub. The solid line and dashed line indicate the transmission characteristic of the resonator with and without additional stub, respectively. Additional stub increases the electrical length of the stub, and an additional resonant mode is shown in the UWB frequency range.
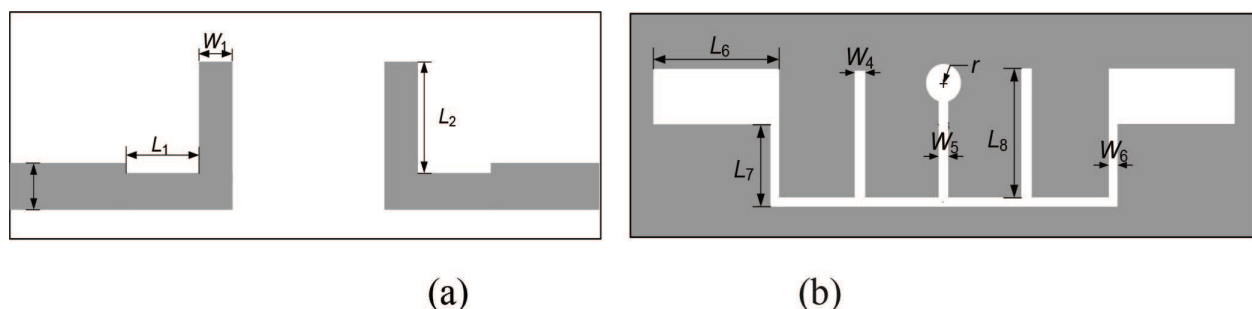

(a)   (b)

Figure 5. Configurations of the proposed UWB filter with three-stub-loaded slot-line MMR. (a) Top view and (b) bottom view.
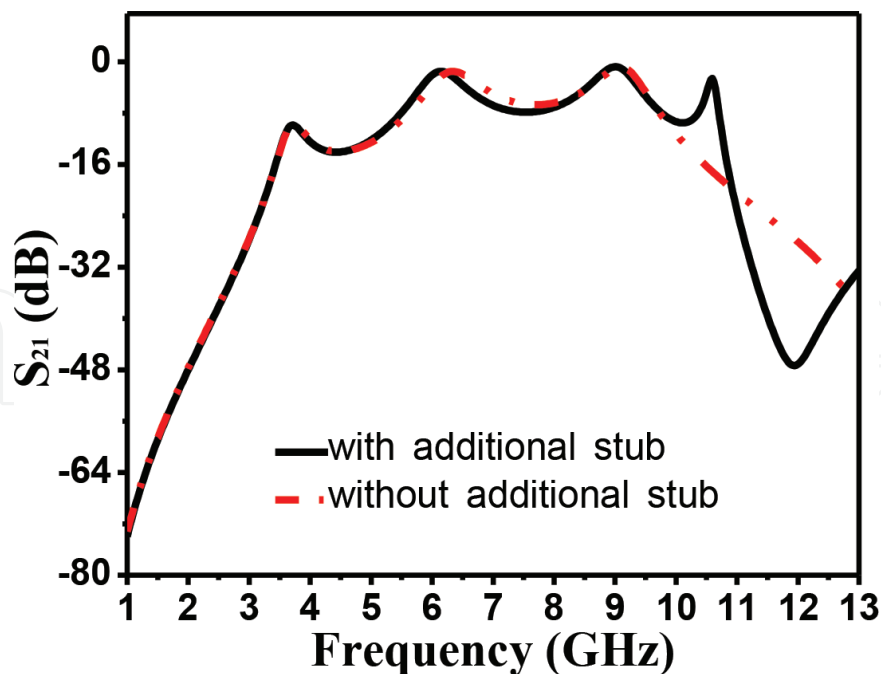
Figure 6. Characteristics of the slot-line MMR with and without the additional stub.

Next, the influence of two parameters of the resonator on the resonant mode of the resonator is studied. **Figure 7** shows the variation of resonant-mode frequencies against L_8, length of the stub, and r, radius of the additional stub. As can be seen from **Figure 7**, four resonant modes (i.e., f_1, f_2, f_3, and f_4) are created in the studied frequency range, which are applied to generate the UWB transmission characteristic. **Figure 7(a)** shows the variation of resonant mode against the length of the stub. As L_8 increases from 2.8 to 4.8 mm, f_3 drops from 10.5 to 8 GHz, and f_4 drops from 11.5 to 10 GHz, which are located in the UWB range, while f_1 and f_2 keep almost unchanged. **Figure 7(b)** depicts the variation of resonant-mode frequencies against the radius of the additional stub. As r increases from 0.4 to 1.0 mm, f_1, f_2, and f_3 remain stationary, while f_4 drops from 12.5 to 10.5 GHz. These resonant frequencies are basically related to the stepped-impedance resonator, and some ones also can be separately controlled by tuning the loaded stubs, which shows great convenience in relocating the required resonant modes of the resonator.

3.2. Band-notched UWB BPF

Based on the UWB filter mentioned above, a notch band is produced and a band-notched UWB BPF is designed. **Figure 8(a)** illustrates the circuit model of a dual-mode resonator-loaded slot-line, where the white section indicates the slot-line, the gray part is the ground, and the black one is a microstrip dual-mode resonator. Equivalent circuit of dual-mode resonator-loaded slot-line is provided in **Figure 8(b)**. Two resonant modes of the stub-loaded resonator are coupled to the slot-line, providing a bypass for the adjacent signal of its resonance. The degree of separation of two modes determines the bandwidth of the notch band, and the coupling between resonator and slot-line influences the amplitude of the attenuation.
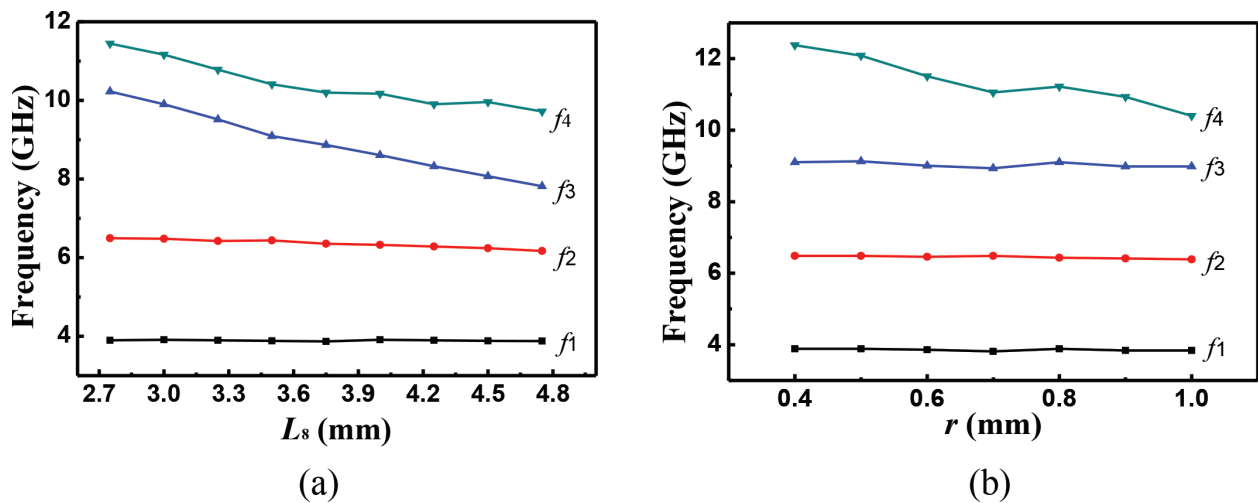
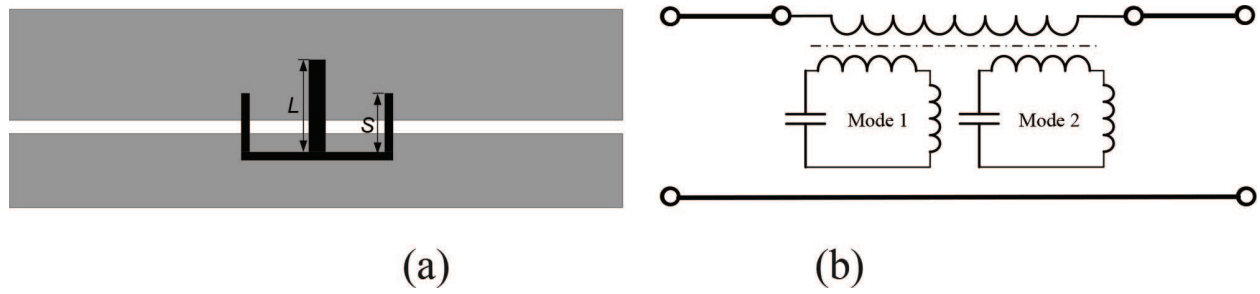**Figure 7.** Resonant-mode frequencies against (a) L_8 and (b) r.

Figure 8. Dual-mode microstrip resonator-loaded slot-line. (a) Structure and (b) its equivalent circuit model.

EM solver is invoked to analyze the relationship between the parameters and the transmission characteristic of the bandstop filter. **Figure 9(a)** shows the transmission characteristics of the resonator versus L, the length of the loading stub. When L increases from 4.5 to 6.0 mm, the lower resonant mode keeps unchanged, and the higher mode decreases from 3.06 to 2.84 GHz.

As we all know that the bandwidth of the bandstop filter is determined by the separation of two poles and the band position of the bandstop filter can be adjusted by the length of the stub L, a transmission pole is also created, which is located near the lower transmission zero, sharping the transition band. **Figure 9(b)** illustrates the effect of varying S on the two modes of the dual-mode resonator. When S increases from 3.0 to 4.5 mm, the bandwidth of the filter increases from 60 to 480 MHz, and the central frequency decreases from 4.6 to 4.2 GHz. Obviously, modifying S and L can change the position and the bandwidth of the stopband.

3.3. Filter implementation and results

Based on the proposed structure, a UWB BPF with notch band from 5.15 to 5.35 GHz is designed and fabricated. The feed lines and the MMR in slot-line are folded and orthogonally coupled to acquire the desired strong coupling. A dual-mode loaded-stub open-loop
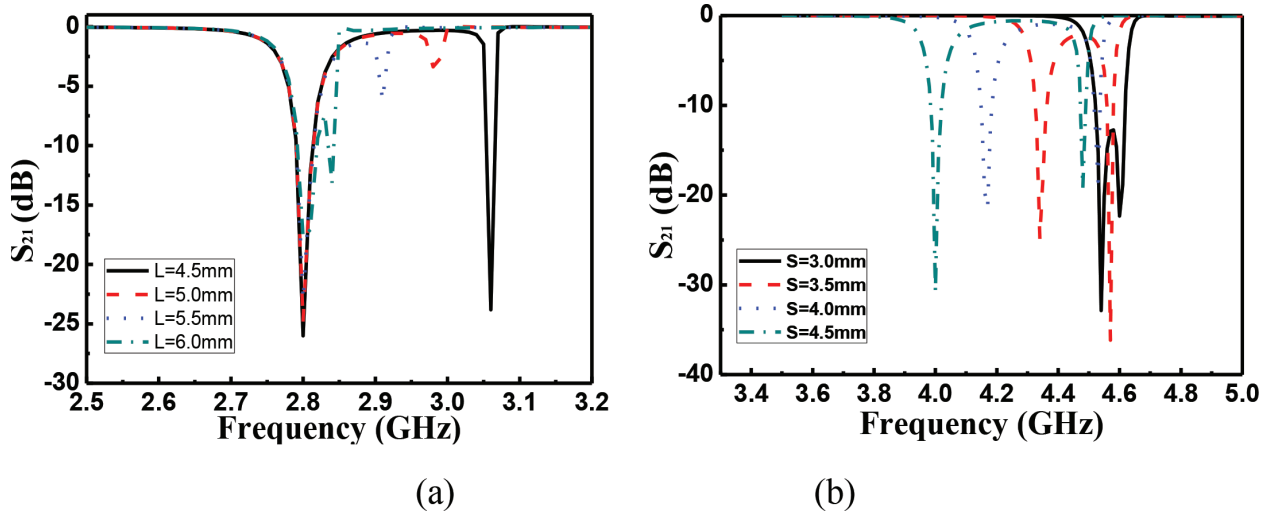
Figure 9. The transmission characteristic of the simplified resonator with varied parameters. (a) L and (b) S.
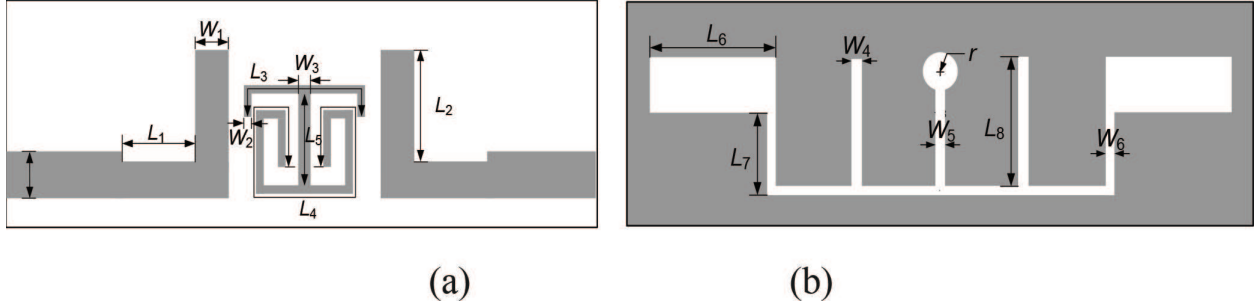

Figure 10. Configurations of the proposed band-notched UWB BPF using dual-mode microstrip resonator-loaded three-stub-loaded slot-line MMR. (a) Top view and (b) bottom view.

resonator is loaded to the slot-line, and a notch band for WLAN is produced, as shown in **Figure 10**. The dual-mode resonator is folded in order to improve the slow-wave effect for miniaturization. A substrate of 28 mm × 18 mm with a relative dielectric constant of $\varepsilon_r = 3.5$ and a thickness of h = 0.8 mm is used in the design. Finally obtained parameters of the filter shown in **Figure 1** are $W_0 = 1.80$ mm, $L_1 = 3.80$ mm, $L_2 = 4.70$ mm, $W_1 = 1.50$ mm, $L_3 = 8.00$ mm, $W_2 = 0.30$ mm, $L_4 = 17.40$ mm, $W_3 = 0.60$ mm, $L_5 = 3.70$ mm, $W_4 = 0.50$ mm, $L_6 = 3.80$ mm, $W_5 = 0.30$ mm, $L_7 = 2.50$ mm, $W_6 = 0.30$ mm, $L_8 = 3.50$ mm, and $r = 0.55$ mm. Measurements are performed by using vector network analyzer AV3926.

A comparison between the simulated and measured results is shown in **Figure 11**, where the solid lines and the dashed lines indicate the EM-simulated results and measured results, respectively. Simulated results show that the 3-dB bandwidth of the filter covers from 3.1 to 5.15 GHz and from 5.35 to 10.6 GHz, while the measured ones show that the 3-dB bandwidth covers from 3.2 to 5.15 GHz and from 5.35 to 10.6 GHz. Simulated and measured insertion losses of each passband are about 2 dB; return losses are −12 dB/−18 dB and − 18 dB/−10 dB. Return loss in the notch band is greater than 15 dB. Except for the deviation that may be caused by the fabrication, the simulated results agree well with the measured results.
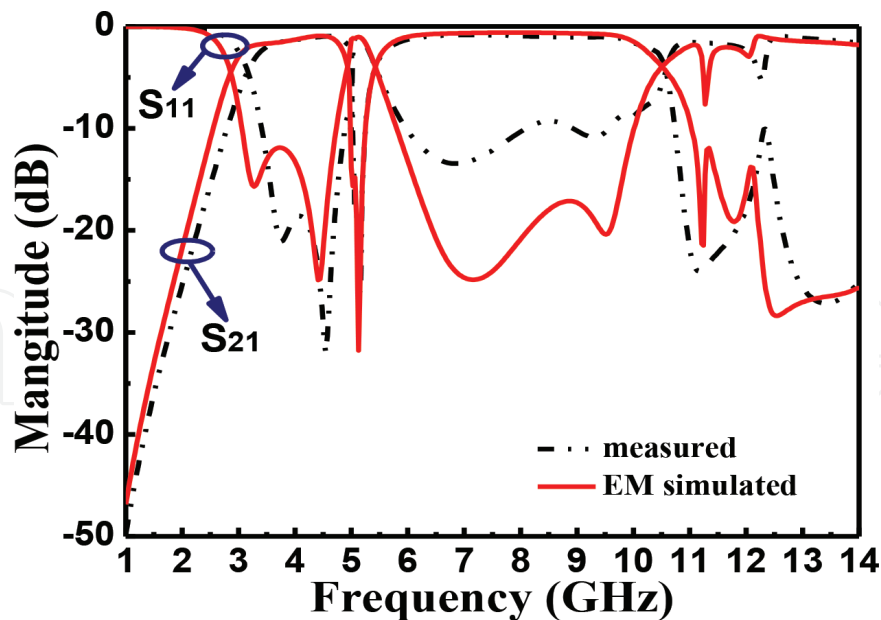
Figure 11. Comparison between measured and EM-simulated results of the band-notched UWB BPF.

4. Triangular loop-loaded band-notched UWB filter

4.1. Dual-stub-loaded slot-line MMR

Two stubs are symmetrically loaded to slot-line, which forms a dual-stub-loaded slot-line MMR, as shown in **Figure 12(a)**. Because the proposed slot-line MMR is a symmetrical structure, even-odd mode theory can be applied to analyze its resonant characteristics. **Figure 12(b)** and **(c)** gives equivalent circuits of the slot-line MMR.

Under odd-mode excitation, the symmetrical plane can be seemed as short-circuited, and its resonant condition can be derived as

$$Z_B \tan \theta_B \tan \theta_C + Z_B \tan \theta_B \tan \theta_A + Z_A \tan \theta_A \tan \theta_C = 0 \qquad (2)$$

where Z_A and Z_B and θ_A, θ_B, and θ_C are the characteristic impedance and electrical length of the dual-stub-loaded MMR, respectively.

Under even-mode excitation, the symmetrical plane can be seemed as open-circuited, and its resonant condition can be summarized as

$$Z_A \tan \theta_A + Z_B \tan \theta_B = Z_B \tan \theta_A \tan \theta_B \tan \theta_C \qquad (3)$$

Resonant modes of the resonator can be controlled and allocated according to the requirements by changing the parameters of the resonator.

To have a clear knowledge of slot-line resonator, resonant characteristics of the dual-stub-loaded slot-line resonator are performed by invoking the 3D EM simulator. Resonant modes
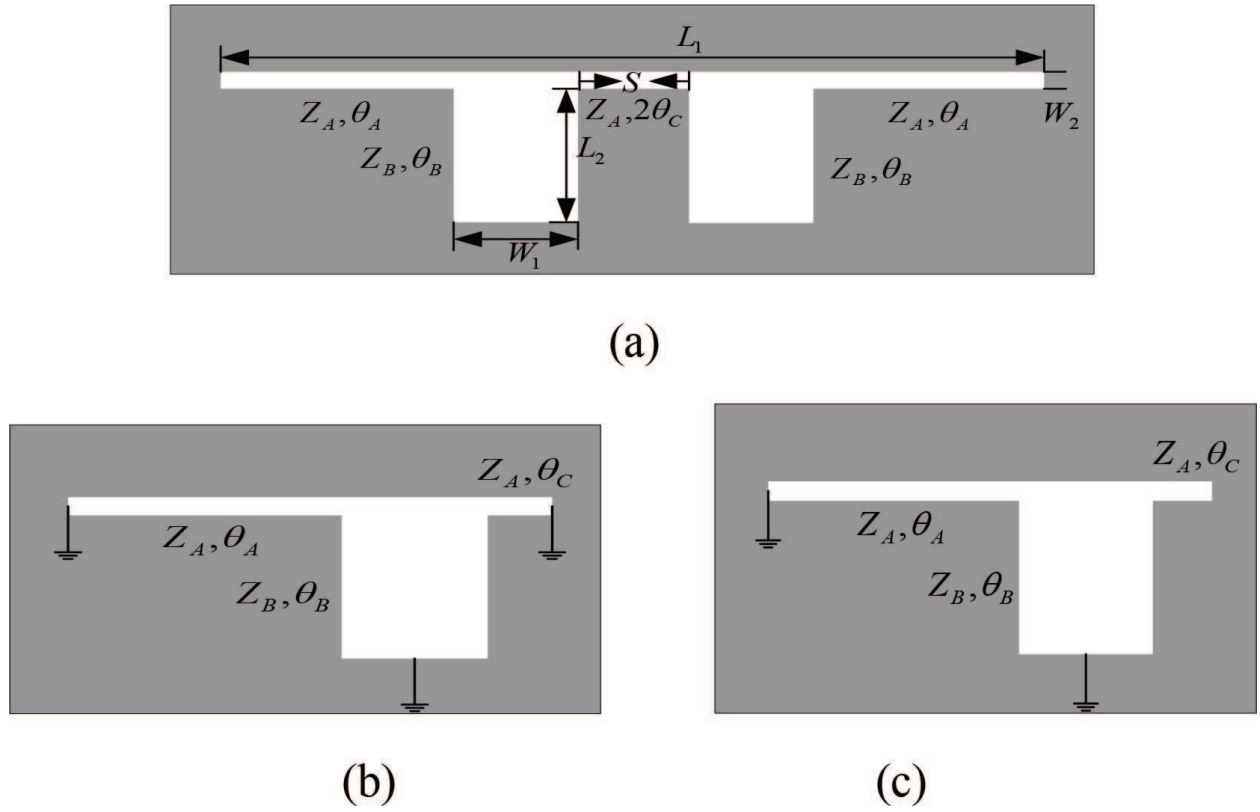
Figure 12. (a) Dual-stub-loaded slot-line MMR and its equivalent circuits: (b) odd mode and (c) even mode.

of slot-line resonator against S, L_1, and L_2 are plotted in **Figure 13**, where f_1, f_2, and f_3 indicate the first, second, and third resonant modes of resonator, respectively. When S increases from 0.2 to 2.2 mm, f_3 decreases from 9.6 to 8.2 GHz, while f_1 and f_2 shift slightly. When L_1 increases from 23 to 25 mm, both f_1 and f_2, together with f_3 decrease steadily. When L_2 increases from 1 to 6 mm, f_2 drops from 8.2 to 6.5 GHz, f_3 drops from 13.5 to 8 GHz, and f_1 keeps unchanged. Obviously, three resonant modes of the resonator can be designed intuitively and well set in the UWB passband.

4.2. Ultra-wideband BPF using dual-stub-loaded slot-line MMR

Layout of a proposed UWB BPF is depicted in **Figure 14**, which is constructed by a slot-line resonator and two microstrip feed lines. On the bottom layer, a dual-stub-loaded slot-line resonator is formed firstly, where two identical stubs are symmetrically loaded to a uniform slot-line resonator. **Figure 15** illustrates the frequency responses of the slot-line UWB BPF with different lengths of feed line (L4) under all the other sizes fixed. When the slot-line resonator is fed under weak coupling case with L_4 = 4.8 mm, three resonant modes with peak S21 magnitudes are observed at about 4.08, 6.41, and 9.5 GHz, respectively. As L_4 increases to 10 mm, the S21 magnitude realizes an almost flat frequency response over a UWB passband. After its sizes are slightly adjusted, an UWB frequency response is satisfactorily realized. Under the use of this hybrid microstrip/slot-line structure, the desired strong coupling between feed lines and MMR can be easily achieved by properly selecting the relative position between them.
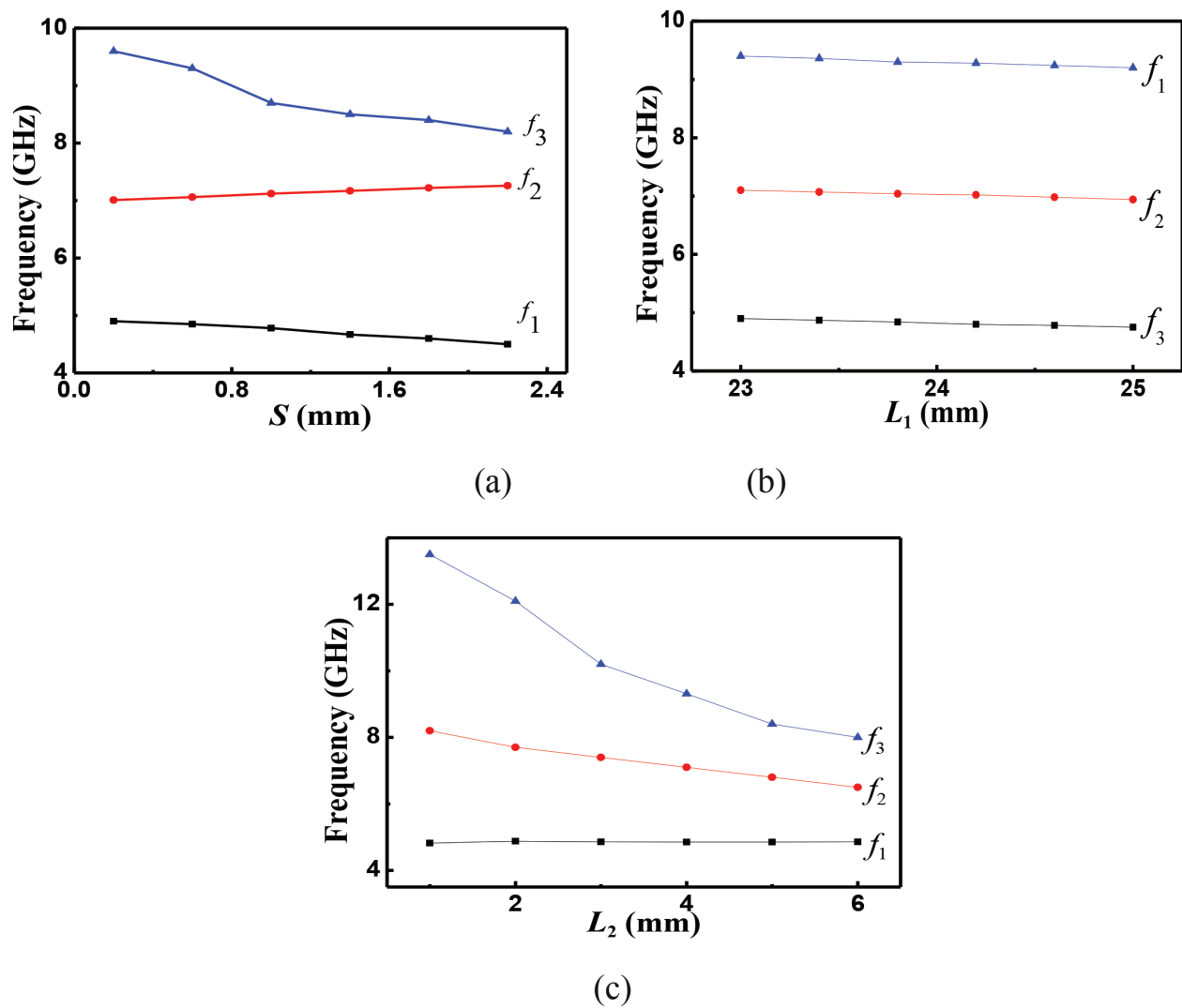
(a)   (b)

(c)

Figure 13. Resonant modes of dual-stub-loaded slot-line resonator with fixed $W_1 = 2.0$ mm, $W_2 = 0.3$ mm, and varied (a) S ($L_1 = 23$ mm, $L_2 = 3$ mm), (b) L_1 ($S = 0.6$ mm, $L_2 = 3$ mm), and (c) L_2 ($S = 0.6$ mm, $L_1 = 23$ mm).
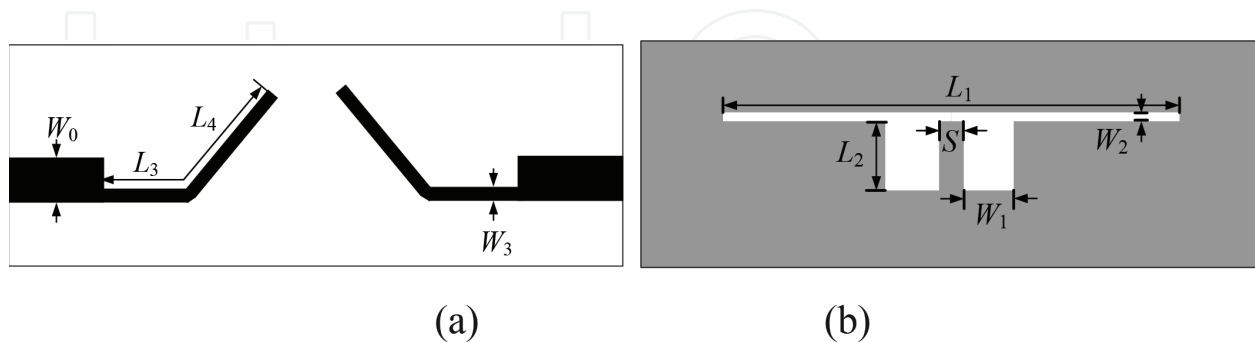

(a)   (b)

Figure 14. Schematic of the UWB BPF using dual-stub-loaded slot-line MMR. (a) Top layer and (b) bottom layer.

4.3. Realization of notch band

Considering the fact that the above-achieved UWB passband range may interfere with the existing wireless systems such as wireless local area network (WLAN), a notch band may be

highly demanded in various practical applications. For this purpose, a microstrip dual-mode triangular loop resonator is formed on the top layer of a dielectric substrate and loaded to the dual-stub-loaded slot-line MMR.

Figure 16 depicts the geometry, equivalent circuit model, and simulated frequency response of a slot-line loaded with back-sided microstrip triangular loop resonator, respectively. **Figure 16(a)** shows a simplified circuit geometry of the structure, where the white portion indicates the slot-line and the black ones are microstrip feed lines and a dual-mode triangular loop resonator with perturbations. Its equivalent circuit model is given in **Figure 16(b)**. Coupling between dual-mode resonator and source/load can be intuitively neglected because its value is quite small. **Figure 16(c)** plots the simulated results derived from the equivalent circuit model, where the solid and dashed lines indicate the simulated reflection and transmission coefficients, respectively. Two transmission zeros in the notch band are created by the resonant modes of the microstrip resonator.

Next, two small patches are symmetrically added as the perturbation element to the lower angles of the triangular loop resonator. These perturbations can accomplish the further separation of the two degenerate modes, creating the dual-mode behavior of the resonator. Resonant modes of the triangular loop resonator are coupled to the slot-line, providing a bypass for the adjacent signal of its resonance, and a notch band is thus created. **Figure 17(a)** shows the transmission characteristics of the resonator versus L_5, that is, the perimeter of a triangular loop resonator. As L_5 increases from 31 to 37 mm, the central frequency of notch band falls off from 6.25 to 5.39 GHz, and its absolute bandwidth decreases from 1.49 to 1.37 GHz. Obviously, the perimeter of triangular loop resonator can directly determine the position of the notch band. **Figure 17(b)** illustrates the influence on the frequency response from varied W_5 and width of two patches. As W_5 increases from 0.2 to 1.0 mm, the notch bandwidth goes up from 1.52 to 1.79 GHz. These exhibited characteristics can be used to determine the central frequency and bandwidth of the created notch band; thus the notch band of the UWB BPF can be fully controlled.
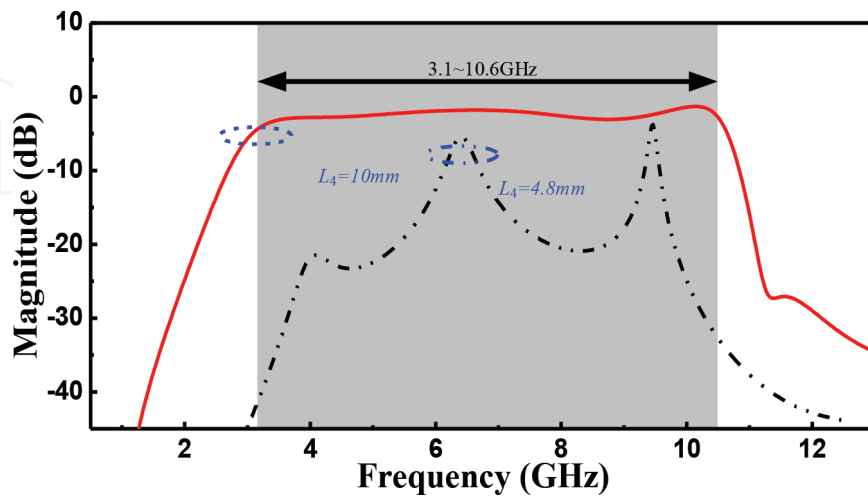

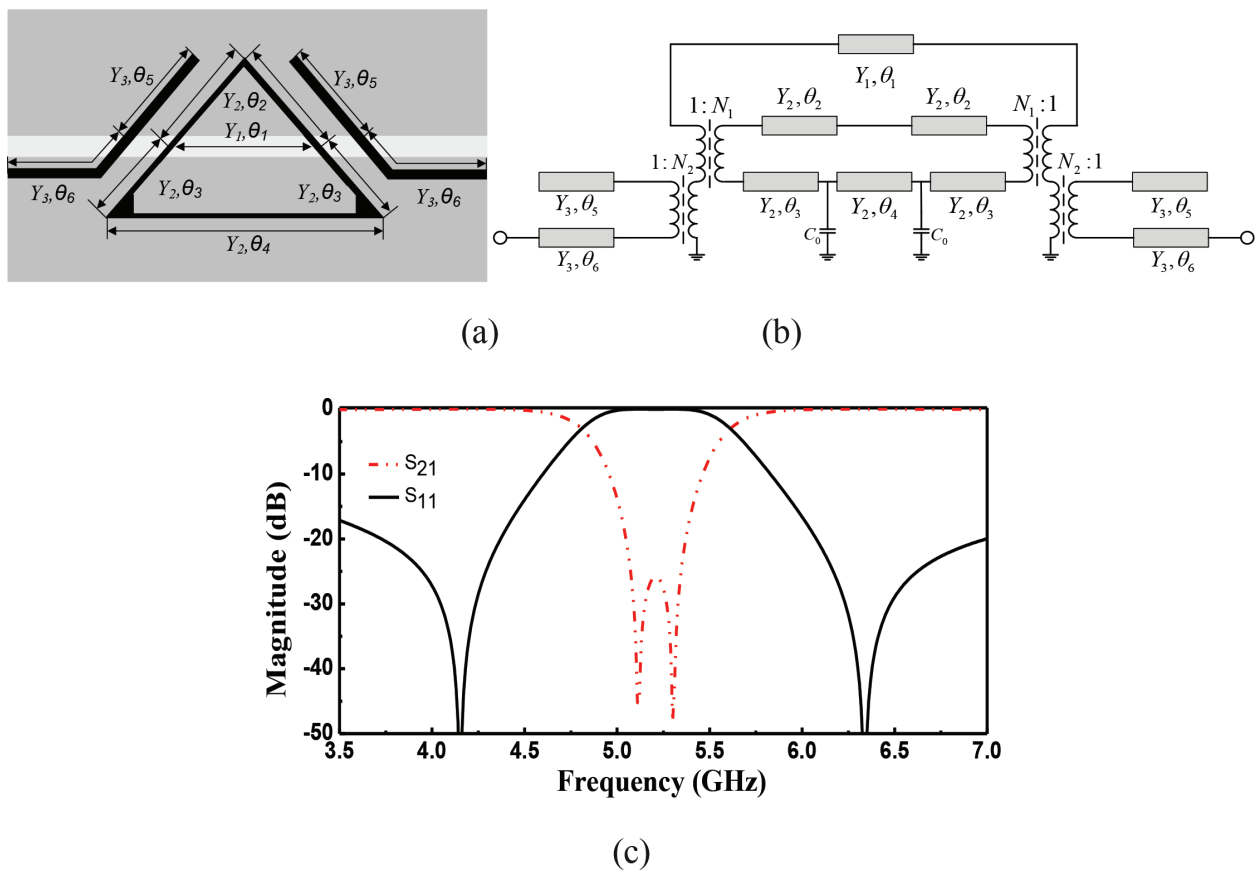**Figure 15.** Frequency responses of transmission coefficient of the proposed UWB BPF with different feeding line lengths (L_4).

(a)   (b)

(c)

Figure 16. A microstrip triangular loop resonator-loaded slot-line. (a) Diagram, (b) equivalent circuit model, and (c) simulated results.

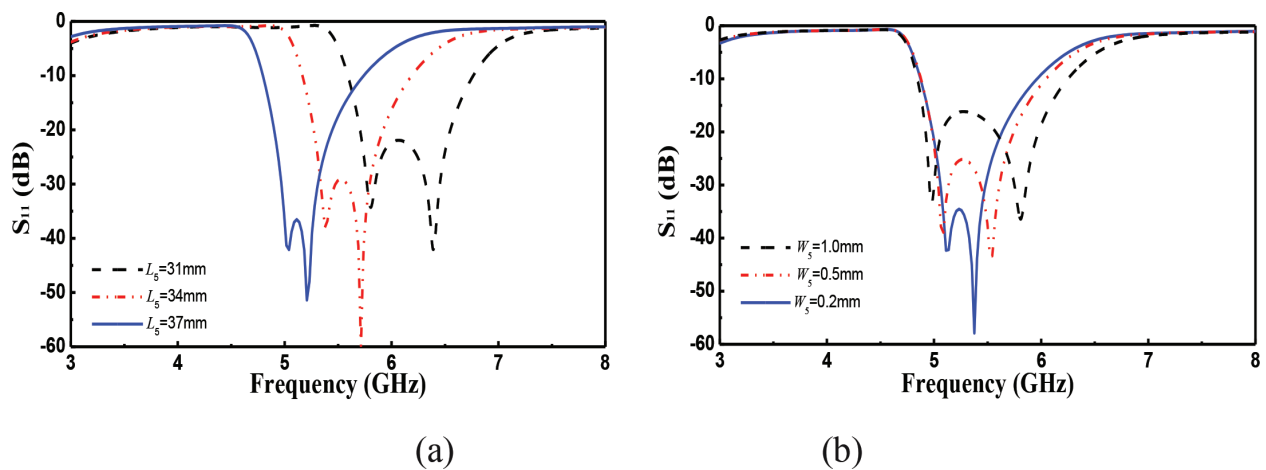(a)   (b)

Figure 17. Frequency-dependent transmission coefficient of the proposed dual-mode triangular loop resonator-loaded slot-line against (a) L_5 and (b) W_5.

4.4. Filter implementation and results

Based on the filter structure and analysis approach described above, a UWB BPF with a controllable notch band is designed and fabricated on a substrate with a dielectric constant of

ε_r = 3.5, loss tangent of 0.0018, and thickness of h = 0.8 mm. The layout of proposed UWB BPF with a notch band is depicted in **Figure 18**. As mentioned above, a dual-stub-loaded slot-line resonator is etched on the ground plane, and on the top layer, two folded microstrip feed lines and a microstrip triangular loop resonator are constructed. All the dimensions of the filter shown in **Figure 18** are W_0 = 1.8 mm, L_1 = 23.0 mm, W_1 = 2.0 mm, L_2 = 3.0 mm, W_2 = 0.3 mm, L_3 = 2.0 mm, W_3 = 0.8 mm, L_4 = 11.5 mm, W_4 = 0.6 mm, L_5 = 36 mm, W_5 = 0.3 mm, and S = 0.6 mm.

Simulated and measured transmission and reflection coefficients of the constructed filter are plotted in **Figure 19**. Simulated results show that the 3-dB passband of the filter covers the ranges of 2.83–4.78 GHz and 6.29–10.33 GHz, respectively, while measured ones show that the 3-dB passband covers the ranges of 2.49–4.91 and 6.29–9.2 GHz. Measured minimum insertion losses of the first and second passband are 1.1 and 1.5 dB, respectively. Measured maximum return losses in the first and second passband are 13.2 and 13.5 dB, respectively. Simulated and measured maximum insertion loss in the notch band is 25 and 35 dB,
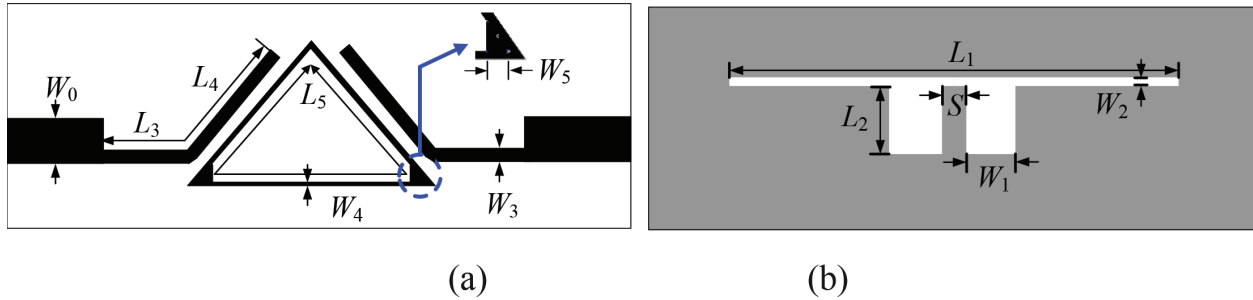

(a)   (b)

Figure 18. Schematic of the proposed band-notched UWB BPF with dual-mode triangular loop resonator-loaded dual-stub slot-line MMR. (a) Top layer and (b) bottom layer.
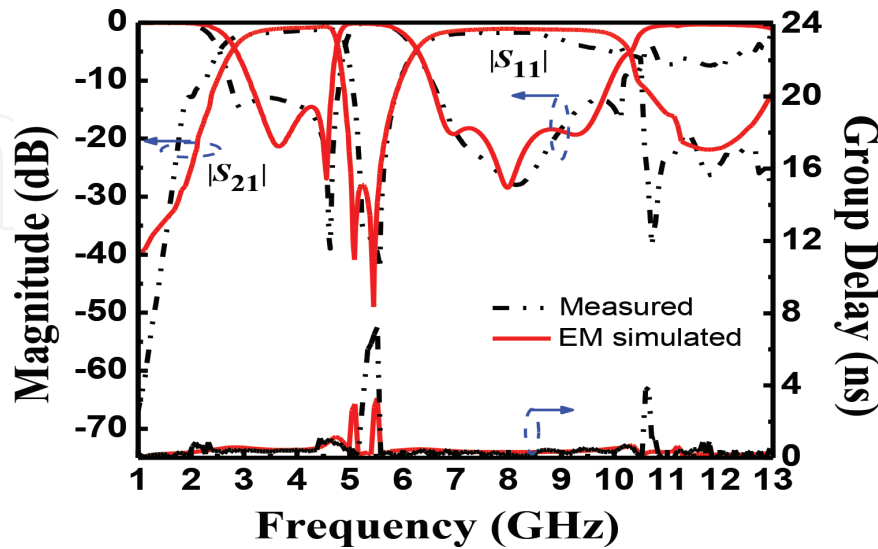

Figure 19. Simulated and measured frequency responses of the designed band-notched UWB BPF.

respectively. In general, the measured results agree well with the simulated results except the loss in the high-frequency band that may be caused by the dielectric loss and fabrication tolerance. Meanwhile, simulated and measured results indicate that the group delay within the passbands is varied between 0.3 and 0.7 ns.

5. Conclusions

Slot-line UWB BPFs and band-notched UWB filters are presented. UWB BPFs are implemented by using microstrip feed slot-line MMR. To acquire a notch band in the UWB passbands, microstrip resonators are loaded to the slot-line. Circuit model for microstrip resonator-loaded slot-line is given and analyzed. The design methodology has been finally verified by the measured results. Band-notched UBW BPFs are hot spots in a few years; there are some trends in this field, such as multiple notched band and tunable notched band.

Author details

Xuehui Guan

Address all correspondence to: xuehuiguan@gmail.com

East China Jiaotong University, Nanchang, PR China

References

[1] Federal Communications Commission. Revision of part 15 of the commission's rules regarding ultra-wideband transmission systems. Tech. Rep., ET-Docket 98-153, FCC02-48. Apr 2002

[2] Zhu L, Sun S, Menzel W. Ultra-wideband (UWB) bandpass filters using multiple-mode resonator. IEEE Microwave and Wireless Components Letters. 2005;**15**(11):796-798

[3] Gao SS, Yang XS, Wang JP, Xiao SQ, Wang BZ. Compact ultra-wideband (UWB) band-pass filter using modified stepped impedance resonator. Journal of Electromagnetic Waves & Applications. 2008;**22**(22):541-548

[4] Wu HW, Chen YW, Chen YF. New ultra-wideband (UWB) bandpass filter using triangle-ring multi-mode stub-loaded resonator. Microelectronics Journal. 2012;**43**(11):857-862

[5] Zhu L, Wang H. Ultra-wideband bandpass filter on aperture-backed microstrip line. Electronics Letters. 2005;**11**(18):1015-1016

[6] Shi X, Xi X, Liu J, Yang H. Novel ultra-wideband (UWB) bandpass filter using multiple-mode resonator. IEICE Electronics Express. 2016;**13**(11)

[7]　Chen CP, Takakura Y, Nihie H, Ma Z. Design of compact notched UWB filter using coupled external stepped-impedance resonator. In: IEEE MTT-S International Microwave Conference; Boston, America. 2009. pp. 945-948

[8]　Ghatak R, Sarkar P, Mishra RK, Poddar DR. A compact UWB bandpass filter with embedded SIR as band notch structure. IEEE Microwave and Wireless Components Letters. 2011;**21**(5):261-263

[9]　Sun H, Feng C, Huang Y, Wen R, Li J, Chen W, Wen G. Dual-band notch filter based on twist split ring resonators. International Journal of Antennas and Propagation. 2014;**2014**. Article ID 541264

[10]　Yang GM, Jin R, Vittoria C, Harris VG, Sun NX. Small ultra-wideband (UWB) bandpass filter with notched band. IEEE Microwave and Wireless Components Letters. 2008;**18**(3):176-178

[11]　Uikey R, Sangam RS, Prasadu K, Kshetrimayum RS. Novel notched UWB filter using stepped impedance stub loaded microstrip resonator and spurlines. International Journal of Microwave Science and Technology. 2015;**2015**. Article ID 939521

[12]　Sarkar P, Reddy BVK, Pal M, Ghatak R. UWB bandpass filter with broad notch band and ultra-wide upper stopband. In: IEEE MTT-S International Microwave and RF Conference; New Delhi, India. 2013. pp. 1-3

[13]　Huang JQ, Chu QX, Liu CY. Compact UWB filter based on surface-coupled structure with dual notched bands. Progress in Electromagnetics Research. 2010;**106**(4):311-319

[14]　Karthikeyan SS, Kshetrimayum RS. Notched UWB bandpass filter using complementary single split ring resonator. IEICE Electronics Express. 2010;**7**(17):1290-1295